ulisses

UNIVERSITY OF LISBON
INTERDISCIPLINARY STUDIES
ON SUSTAINABLE ENVIRONMENT AND SEAS

ulisses.ulisboa.pt

unite! University Network for Innovation, Technology and Engineering

U LISBOA | UNIVERSIDADE DE LISBOA

Co-funded by the Erasmus+ Programme of the European Union

Ulisses

Unmanned Aerial Vehicles for Environmental Monitoring

Alexandra Moutinho
Control, Automation and Industrial Informatics
Mechanical Engineering Department
Instituto Superior Técnico, Universidade de Lisboa

unite! University Network for Innovation, Technology and Engineering

U LISBOA | UNIVERSIDADE DE LISBOA

Co-funded by the Erasmus+ Programme of the European Union

Ulisses

Module contents

1. Introduction to Unmanned Aerial Systems
2. UAVs payload: sensors for environmental monitoring
3. UAVs operation
4. Examples of application of UAVs for environmental monitoring

unite! University Network for Innovation, Technology and Engineering

U LISBOA | UNIVERSIDADE DE LISBOA

Co-funded by the Erasmus+ Programme of the European Union

Ulisses

Module contents

1. Introduction to Unmanned Aerial Systems
2. **UAVs payload: sensors for environmental monitoring**
3. UAVs operation
4. Examples of application of UAVs for environmental monitoring

unite! University Network for Innovation, Technology and Engineering

U LISBOA | UNIVERSIDADE DE LISBOA

Co-funded by the Erasmus+ Programme of the European Union

Remote sensing

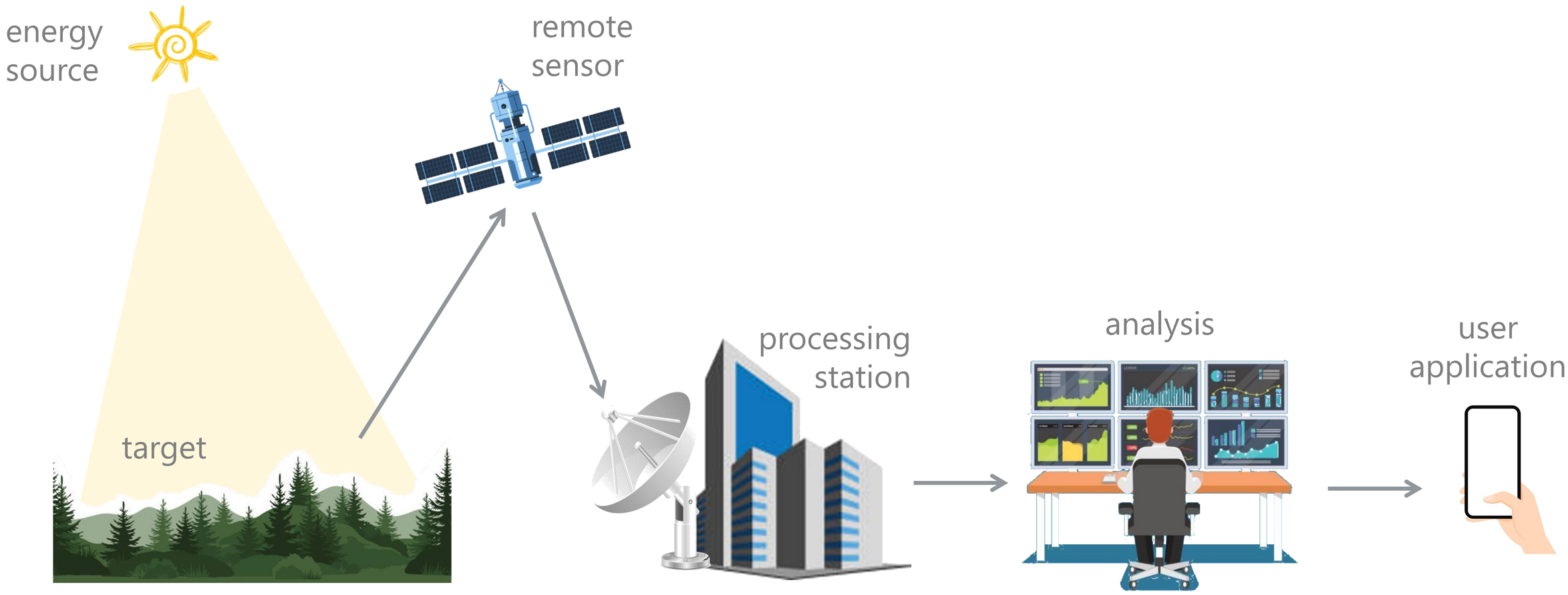

Remote sensing

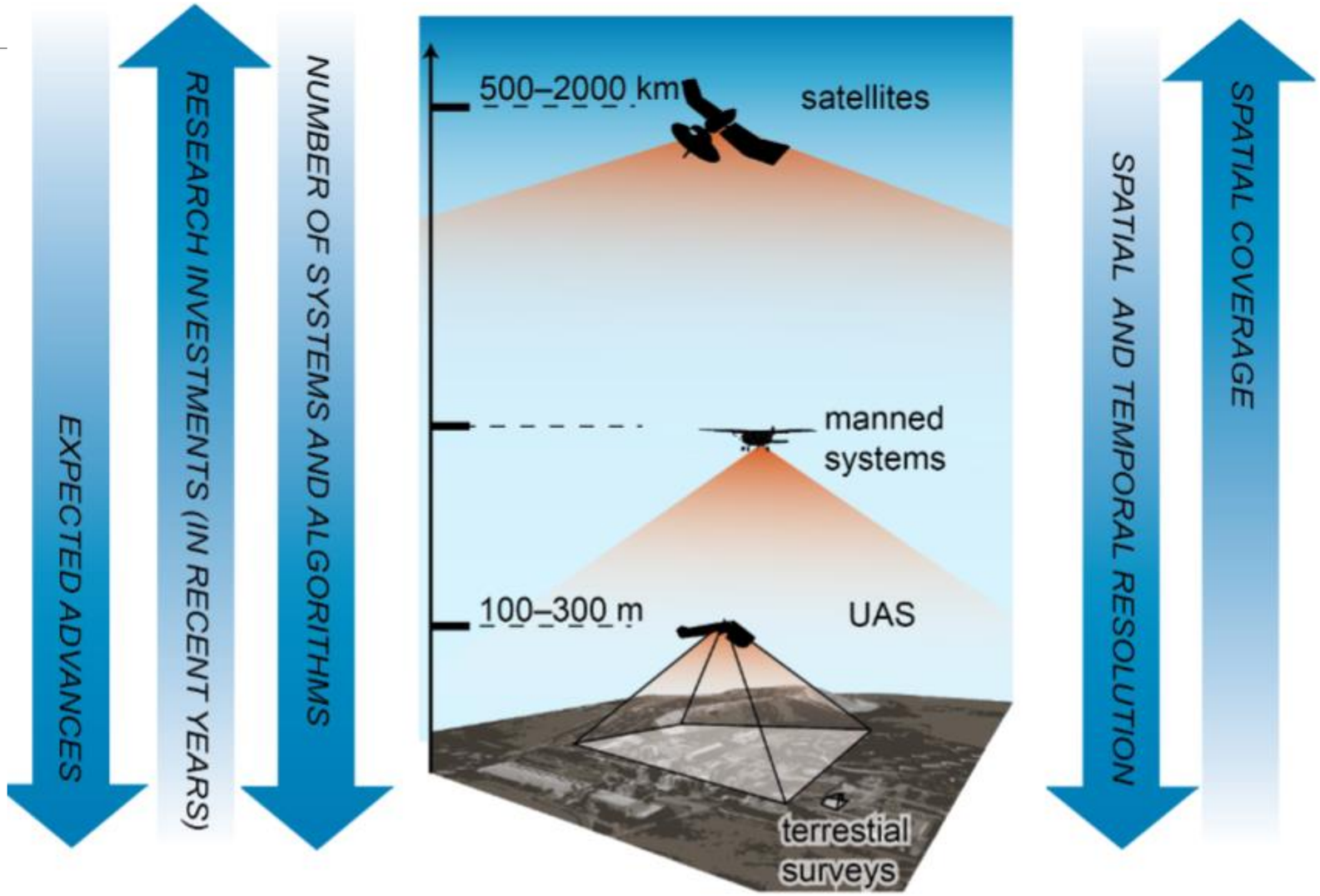

Justyna Jeziorska, UAS for Wetland Mapping and Hydrological Modeling, Remote Sensing, 11, 2019, doi:10.3390/rs11171997

unite! University Network for Innovation, Technology and Engineering

U LISBOA | UNIVERSIDADE DE LISBOA

Co-funded by the Erasmus+ Programme of the European Union

Sensors

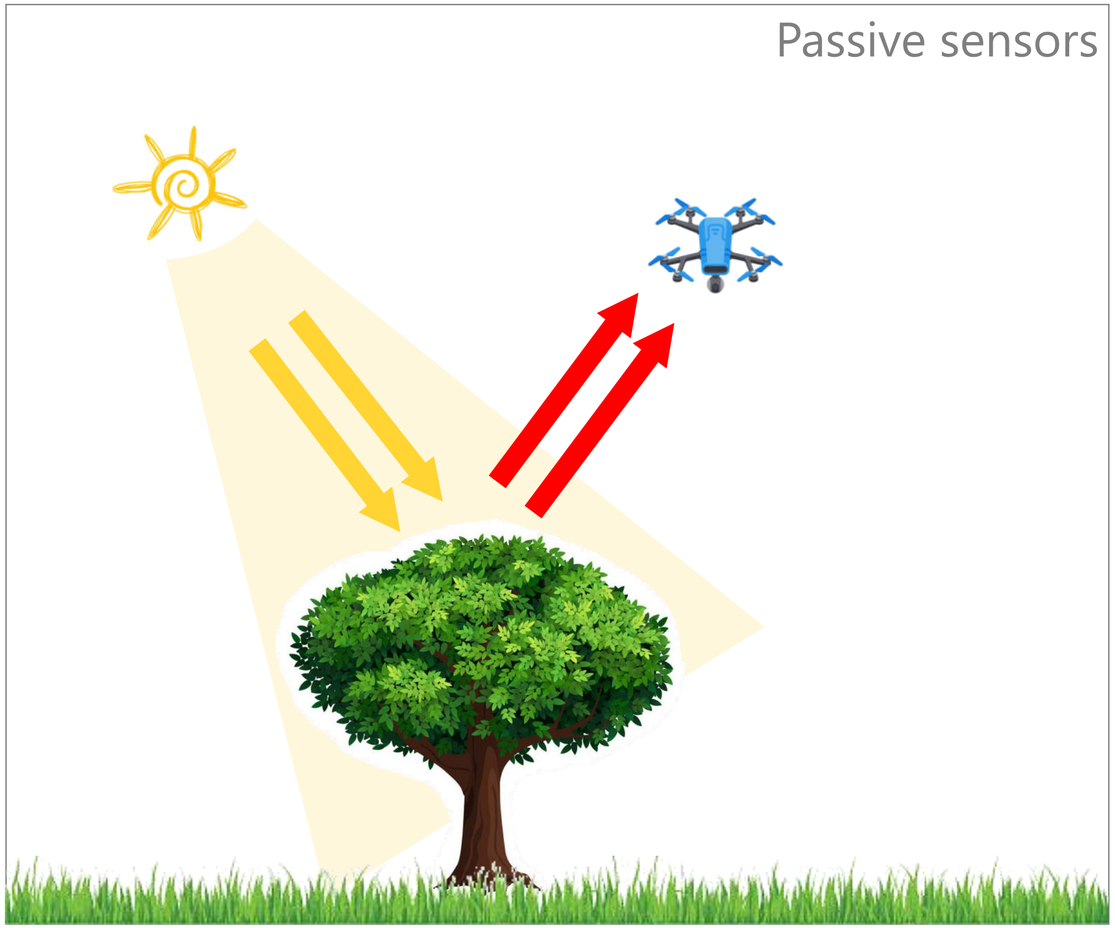

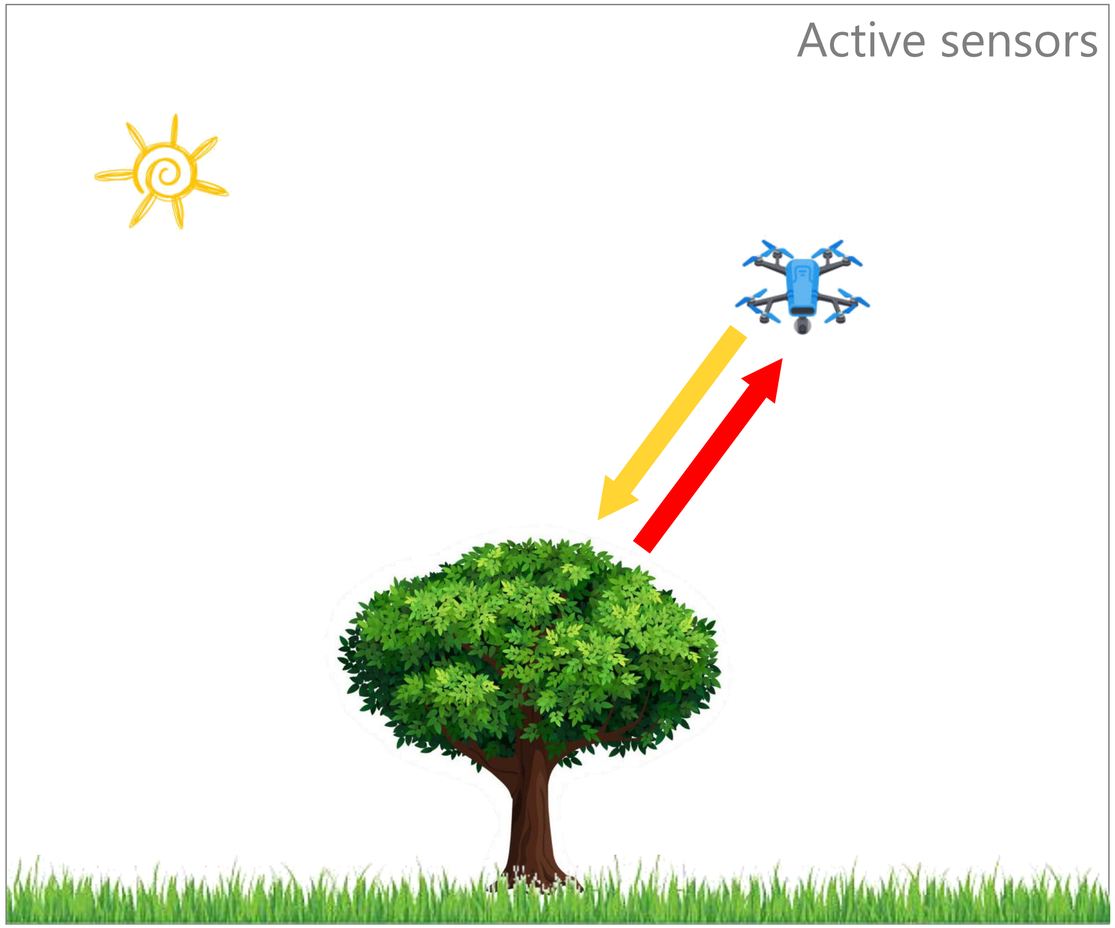

unite! University Network for Innovation, Technology and Engineering

U LISBOA | UNIVERSIDADE DE LISBOA

Co-funded by the Erasmus+ Programme of the European Union

Passive sensors

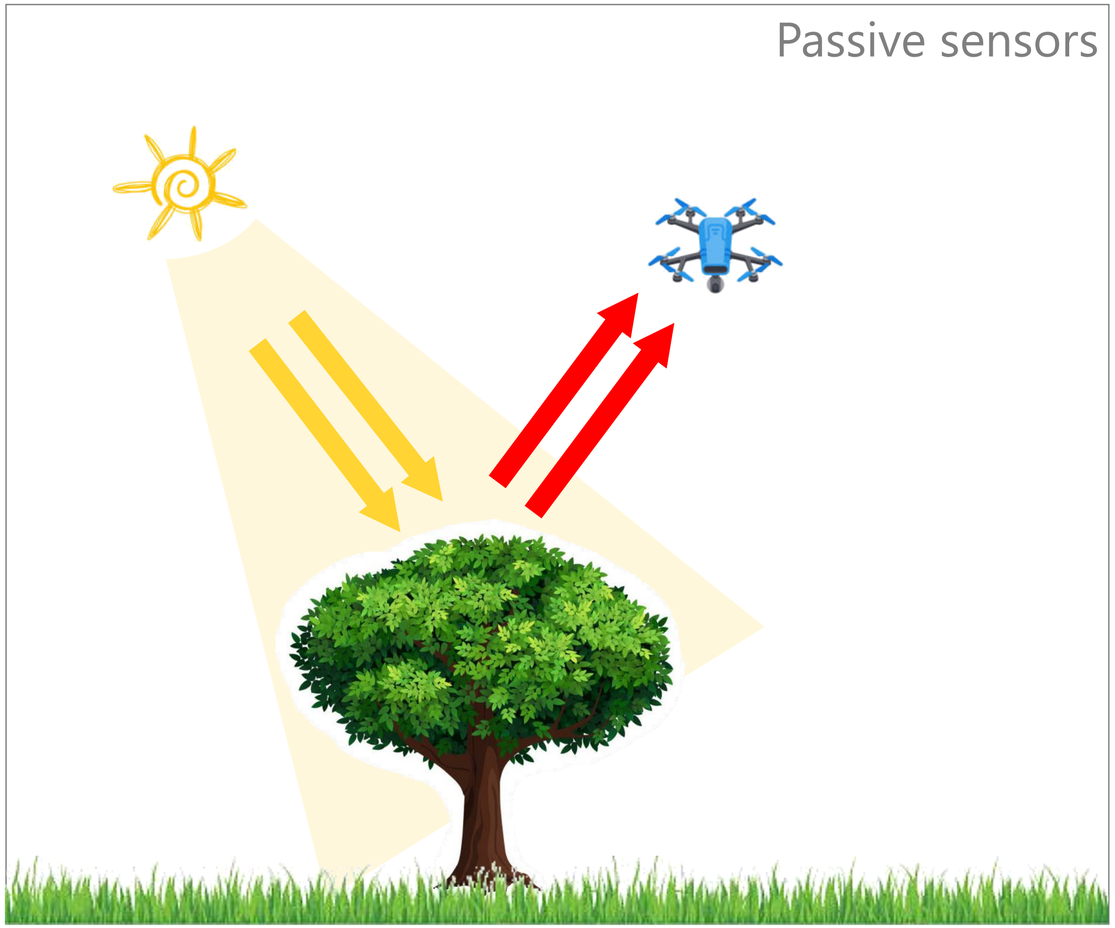

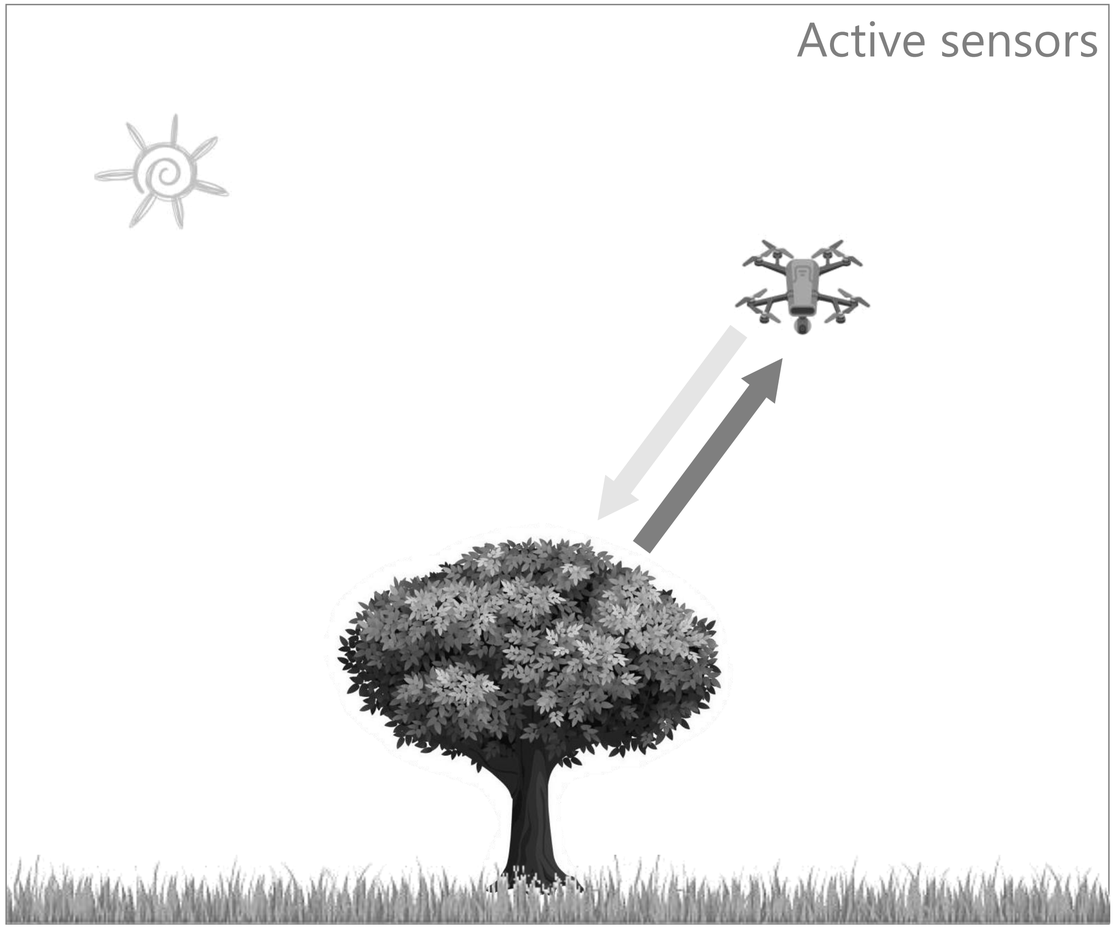

unite! University Network for Innovation, Technology and Engineering

U LISBOA | UNIVERSIDADE DE LISBOA

Co-funded by the Erasmus+ Programme of the European Union

Electromagnetic spectrum

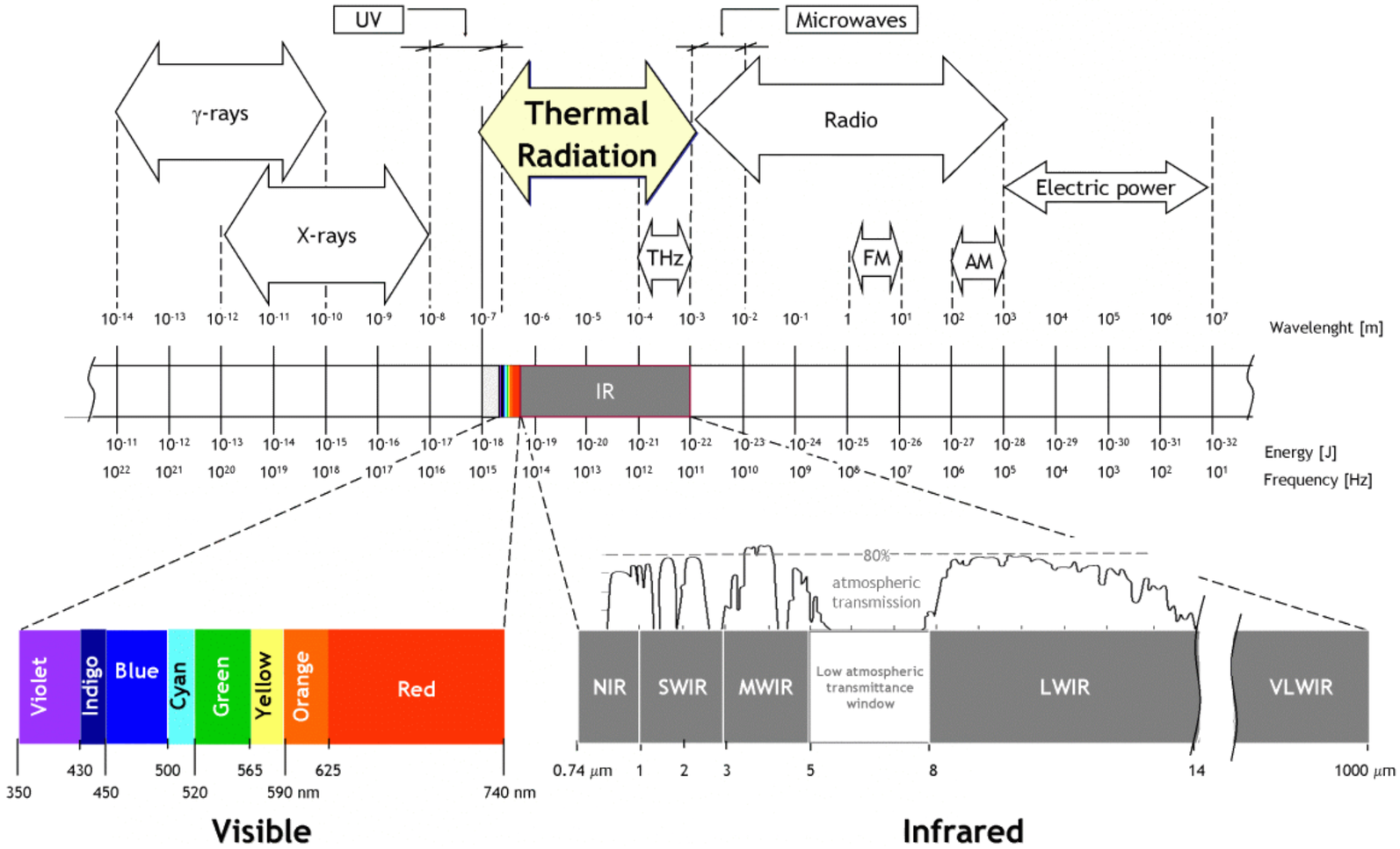

Infrared vision - Wikiwand

Passive sensors

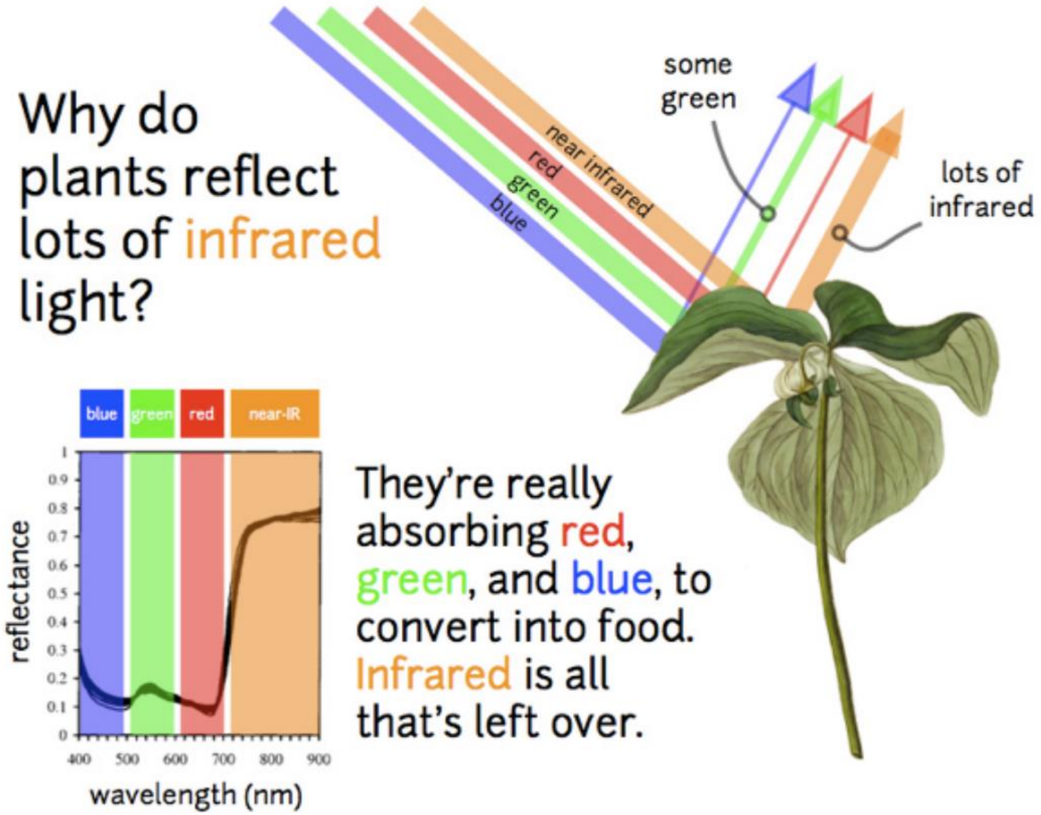

Abigail Sanders, "Unmanned Aerial Vehicles (UAVs) for Remote Sensing and Environmental Monitoring", https://www.eurosite.org/wp-content/uploads/3_Drones_for_remotesensing_and_env_monitoring.pdf

Passive sensors

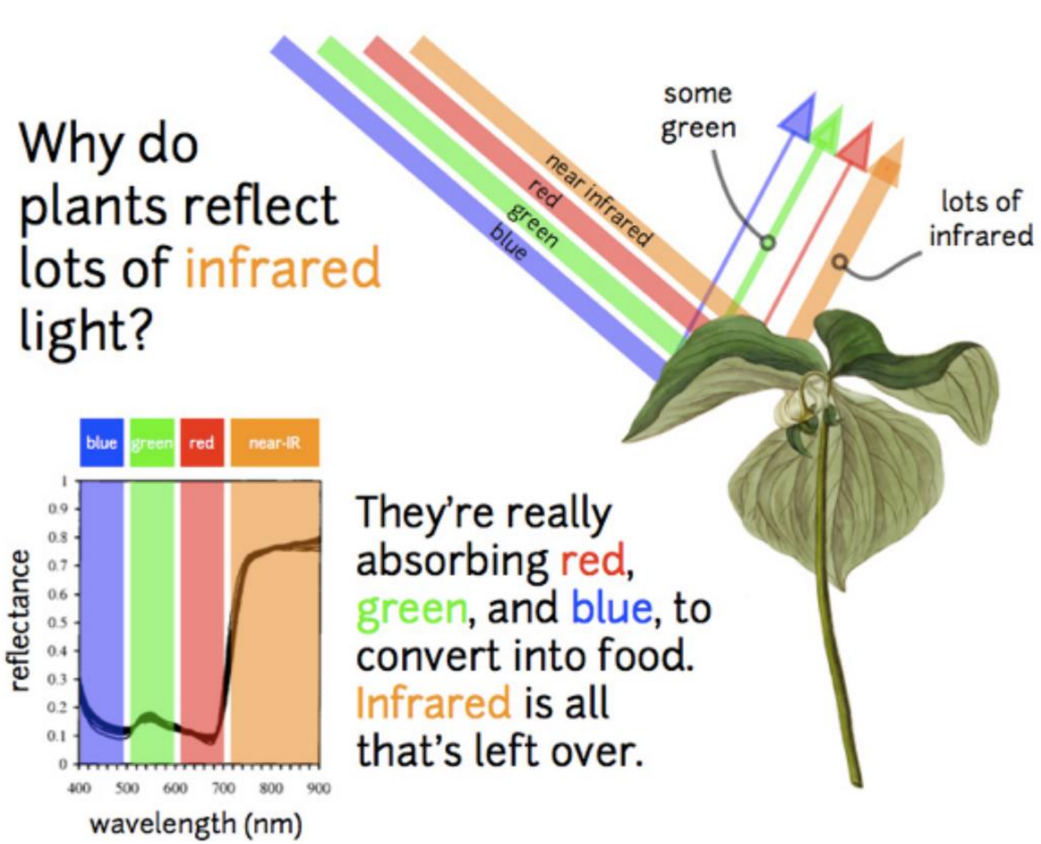

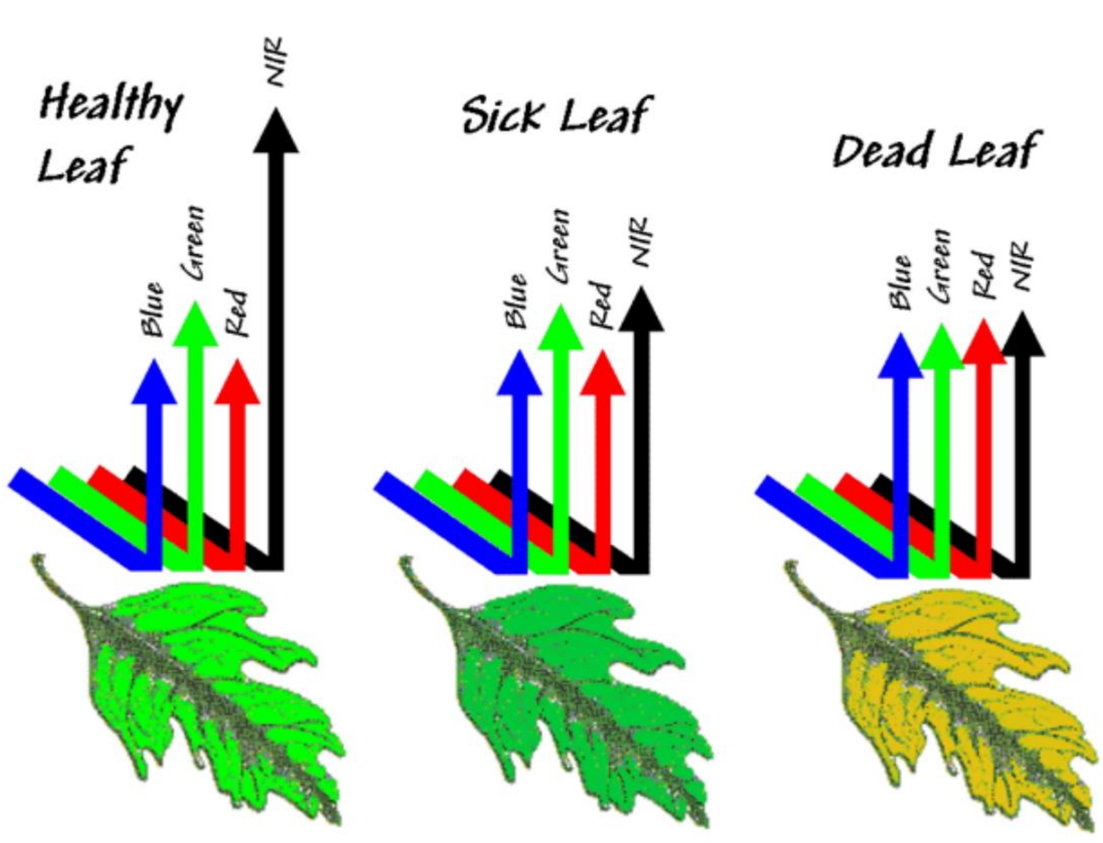

Abigail Sanders, "Unmanned Aerial Vehicles (UAVs) for Remote Sensing and Environmental Monitoring", https://www.eurosite.org/wp-content/uploads/3_Drones_for_remotesensing_and_env_monitoring.pdf

Active sensors

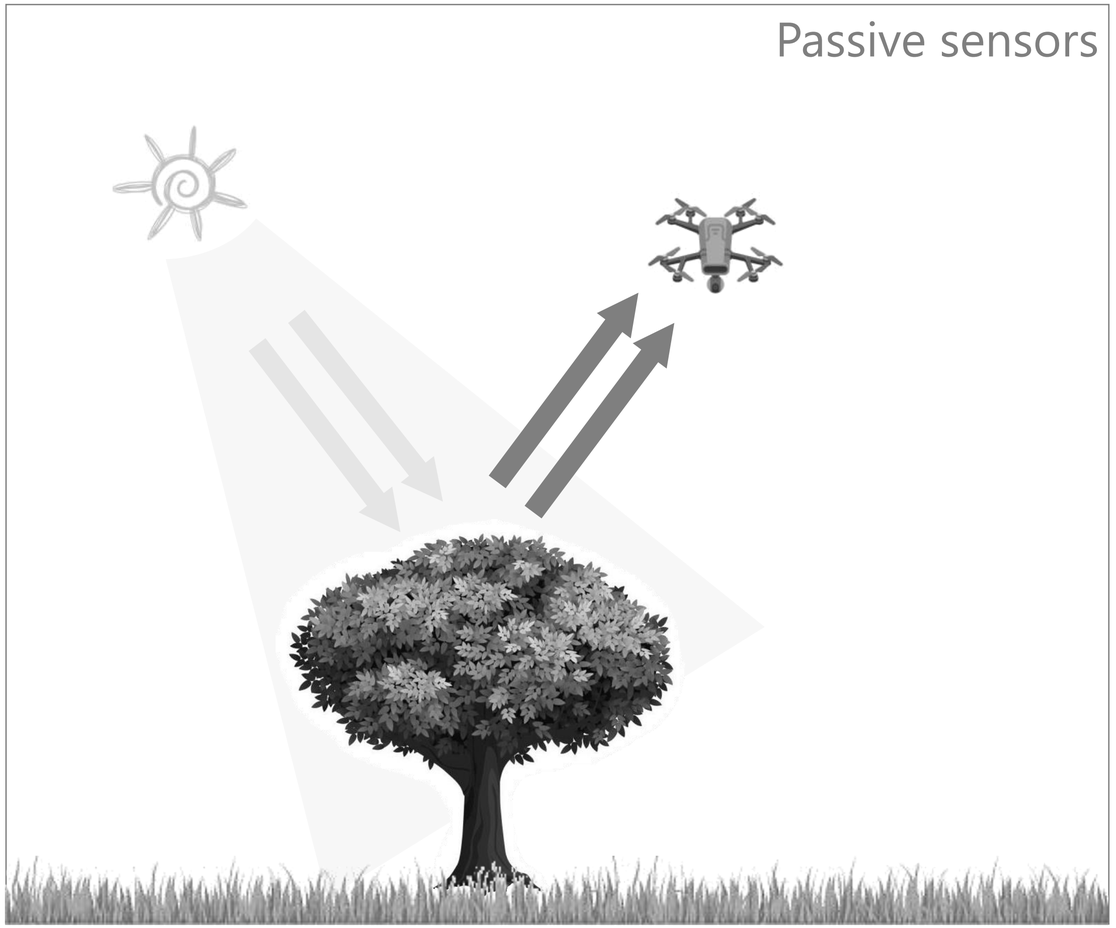

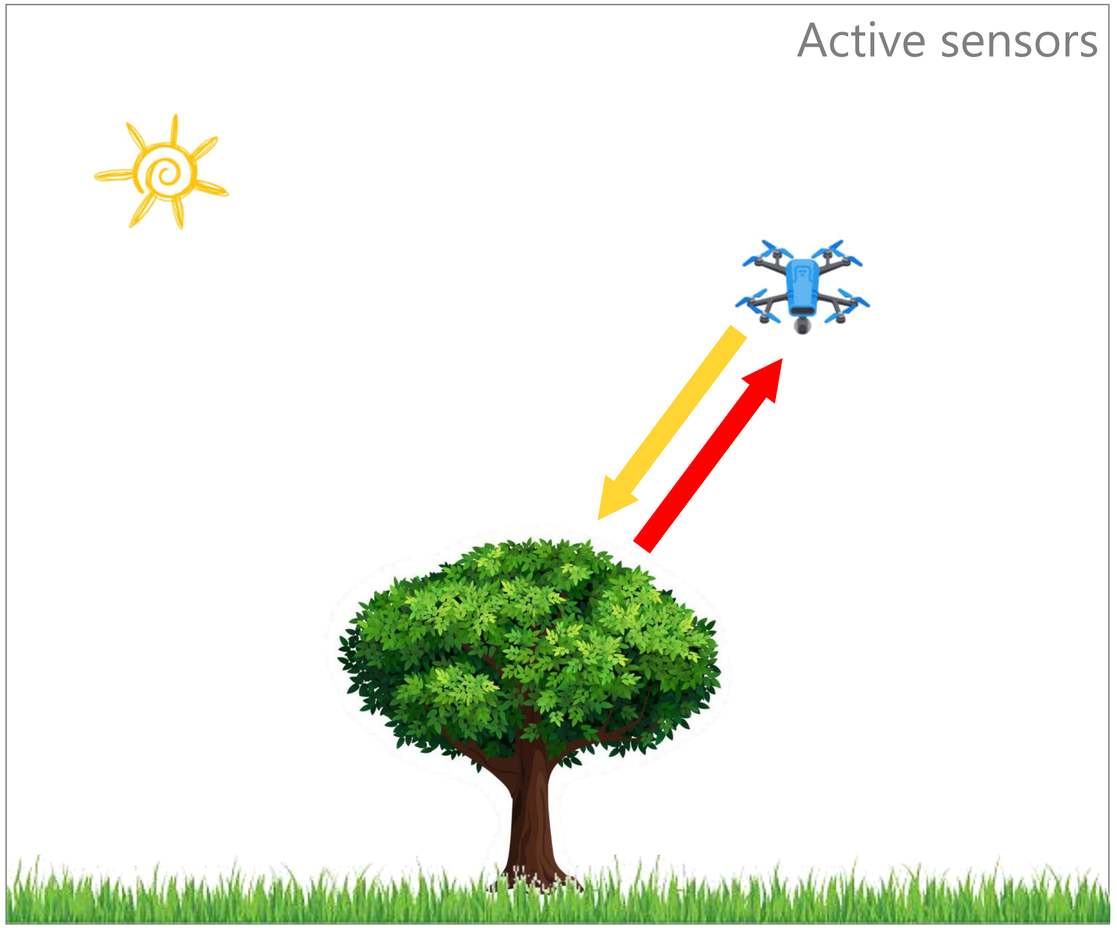

unite! University Network for Innovation, Technology and Engineering

U LISBOA | UNIVERSIDADE DE LISBOA

Co-funded by the Erasmus+ Programme of the European Union

Active sensors

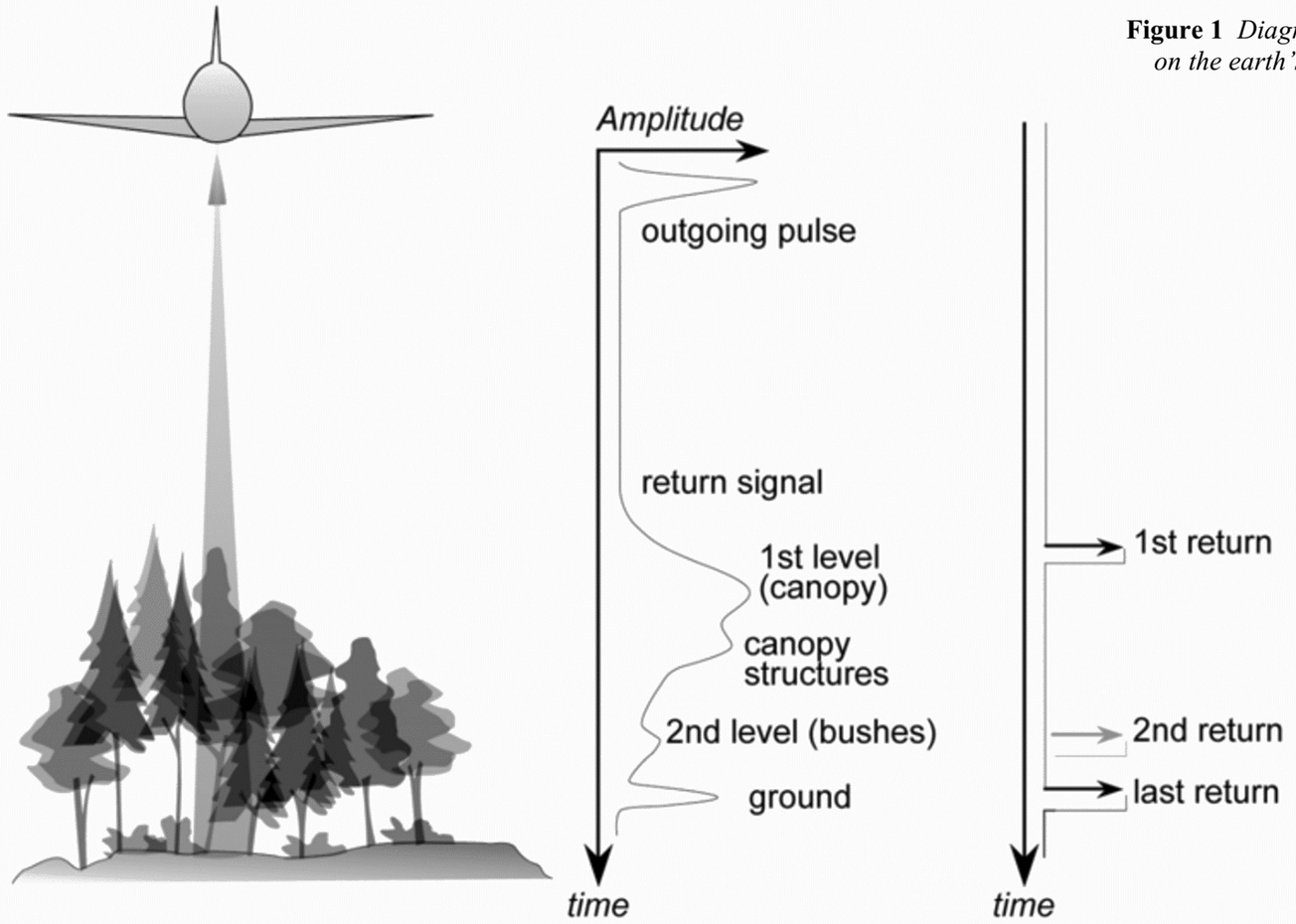

Figure 1 *Diagram showing a typical airborne lidar. Typically, each pulse is reflected from a number of objects on the earth's surface, generating multiple returns that are captured digitally as discrete pulses by the data logging system. The amplitude of each return is logged as the intensity value.*

Challis, K., A. Howard, Derek Moscrop, B. Gearey, David Smith, C. Carey and A. Thompson. "Using airborne LiDAR intensity to predict the organic preservation of waterlogged deposits." (2018).

Active sensors

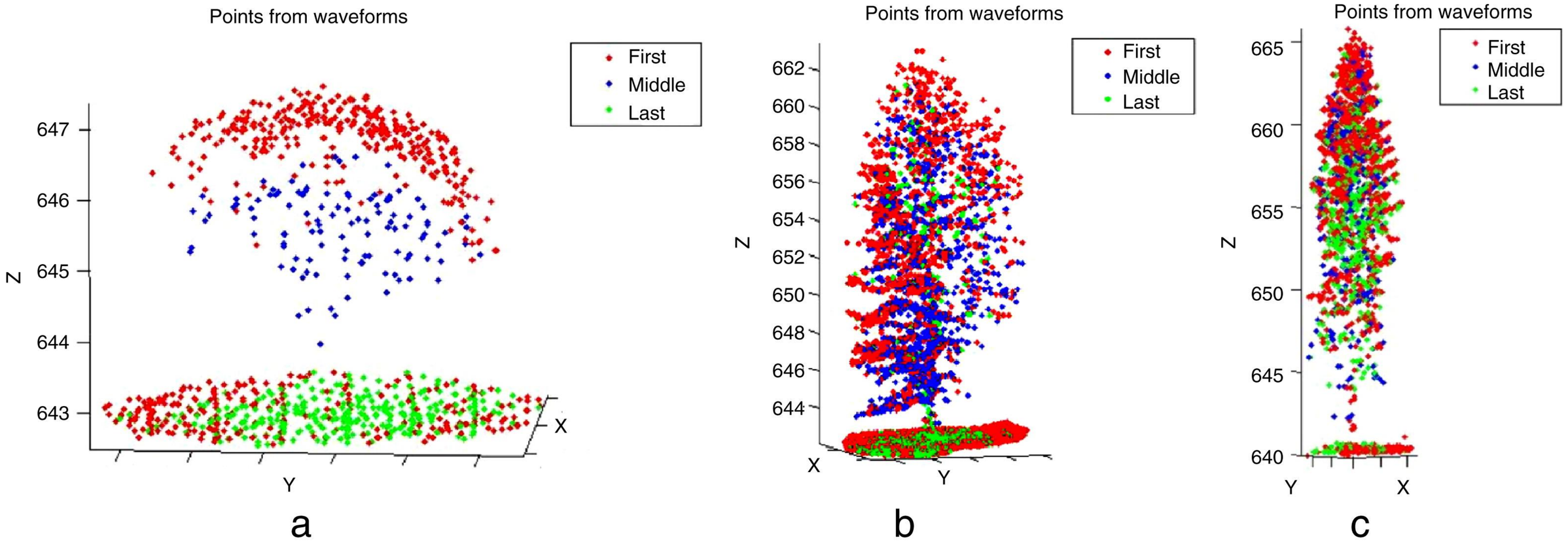

Fig. 6. Extracted points on different tree species from full-waveform data post-processing. (a) Deciduous (leaf-on). (b) Deciduous (leaf-off). (c) Coniferous. Red, green and blue points correspond respectively to the first, last and intermediate extracted pulses (Reitberger et al., 2008a).

Clément Mallet, Frédéric Bretar, Full-waveform topographic lidar: State-of-the-art, ISPRS Journal of Photogrammetry and Remote Sensing, 64(1):1:16, 2009, doi: 10.1016/j.isprsjprs.2008.09.007

Remote sensing

carrier

?

sensing payload

unite! University Network for Innovation, Technology and Engineering

U LISBOA | UNIVERSIDADE DE LISBOA

Co-funded by the Erasmus+ Programme of the European Union

Visual-band cameras

Table 3. Main parameters of some commonly used UAS mounted Visual-Band cameras.

Manufacturer and Model	Resolution [px]	Weight [g]	Speed [/s]
DJI Zenmuse X7	24 MP (multiple photo sizes)	449	up to 6000
MAPIR Survey3	4000 × 3000	50 *	up to 200
PhaseOne iXU-RS 1000	11,608 × 8708	930	up to 2500
Sony ILCE-QX1	5456 × 3632	158 *	up to 4000
senseFly S.O.D.A.	5472 × 3648	111	up to 2000

** Without lens.*

Figure 5. Some commonly used UAS Visual-Band cameras, listed in Table 3: **(A)** DJI Zenmuse X7; **(B)** MAPIR Survey3 (also avaliable in multispectral option); **(C)** PhaseOne iXU-RS 1000; **(D)** Sony ILCE-QX1; **(E)** senseFly S.O.D.A.

Figure 7. Left: High-resolution mosaic, constructed from aerial images acquired by a quadcopter over the Campsite of Côja, overlaying Google Earth. Right: Zoom of the area indicated in red in the image

M. Almeida et al., Analysis of fire hazard in campsite areas, Fire Technology, 53(2):553-575, 2017, doi: 10.1007/s10694-016-0591-5

Justyna Jeziorska, UAS for Wetland Mapping and Hydrological Modeling, Remote Sensing, 11, 2019, doi:10.3390/rs11171997

Visual-band cameras

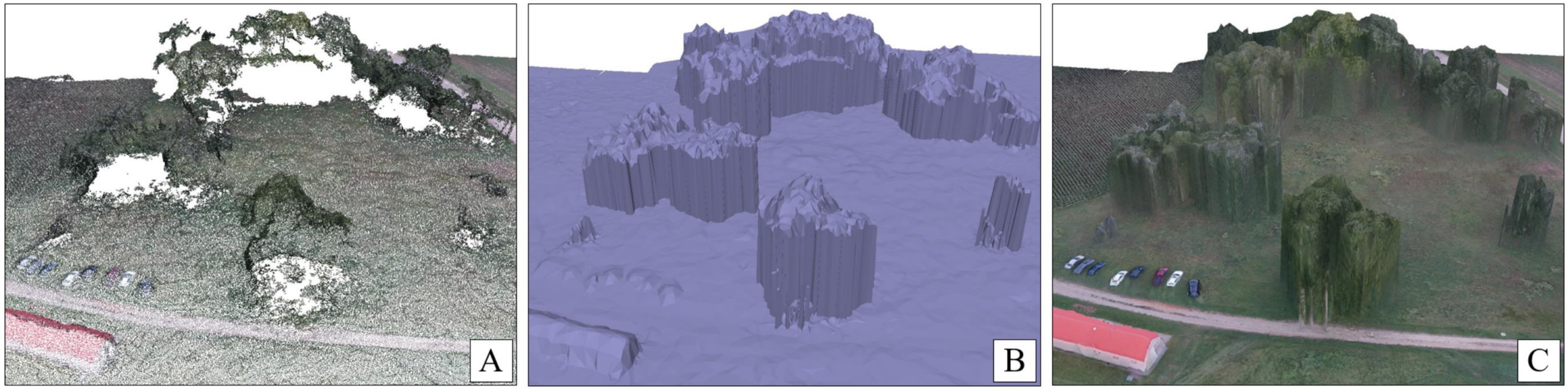

Figure 7. Processed RGB imagery using Structure from Motion (SfM) techniques. Visible lack of data below the canopy on dense point cloud (**A**) and resulting misrepresentation of the canopy structure on a 3D model (**B**) and textured 3D model (**C**).

Justyna Jeziorska, UAS for Wetland Mapping and Hydrological Modeling, Remote Sensing, 11, 2019, doi:10.3390/rs11171997

Thermal cameras

Figure 9. Currently available thermal cameras, listed in Table 6: (**A**) FLIR T450sc; (**B**) FLIR Thermovision A40M; (**C**) ICI 7640 P-Series; (**D**) Optris PI400; (**E**) Pearleye LWIR; (**F**) Thermoteknix MIRICLE 370 K; (**G**) Xenix Gobi-384 (Scientific).

Table 6. Some of the currently available thermal cameras, after Khanal et al. [29], modified.

Manufacturer and Model	Resolution [px]	Weight [g]	Spectral Band [µm]
FLIR T450sc	320 × 240	880 *	7.5–13.0
FLIR Tau 640	640 × 512	110	7.5–13.5
FLIR Thermovision A40M	320 × 240	1400	7.5–13.5
ICI 320x	320 × 240	150 *	7.0–14.0
ICI 7640 P-Series	640 × 480	127.6	7.0–14.0
InfraTec mobileIR M4	160 × 120	265 *	8.0–14.0
Optris PI400	382 × 288	320 *	7.5–13.0
Pearleye LWIR	640 × 480	790 *	8.0–14.0
Photon 320	324 × 256	97	7.5–13.5
Tamarisk 640	640 × 480	121	8.0–14.0
Thermoteknix MIRICLE 370 K	640 × 480	166	8.0–12.0
Xenix Gobi-384 (Scientific)	384 × 288	500 *	8.0–14.0

** With housing and lens.*

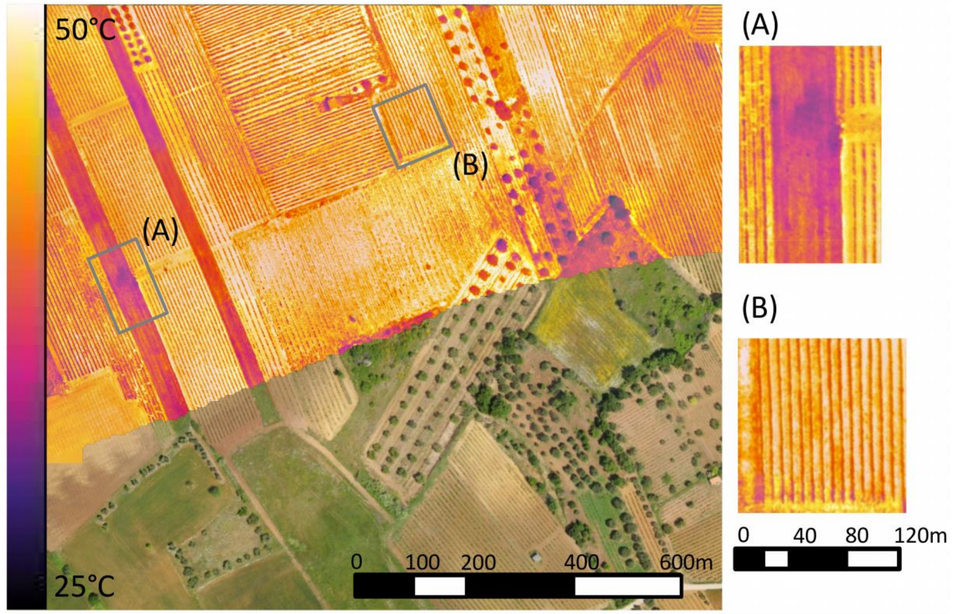

Figure 2. A thermal survey over an Aglianico vineyard in the Basilicata region (southern Italy) overlaying an RGB orthophoto obtained by a multicopter mounted with both optical and FLIR Tau 2 cameras. Insets (**A**) and (**B**) provide magnified portions of the thermal map, where it is possible to distinguish vineyard rows (**B**) and surface temperature distribution on bare soil with a spot of colder temperature due to higher soil water content (**B**).

Justyna Jeziorska, UAS for Wetland Mapping and Hydrological Modeling, *Remote Sensing*, 11, 2019, doi:10.3390/rs11171997

Salvatore Manfreda et al., On the use of unmanned aerial systems for environmental monitoring, Remote Sensing, 2018, 10, 641, doi:10.3390/rs10040641

LiDAR

Figure 10. Some commonly used lidar sensors for UAS, listed in Table 7: (**A**) Riegl VUX-1UAV; (**B**) Riegl VUX-240; (**C**) Routescene UAV LidarPod; (**D**) Velodyne HDL-32E; (**E**) Velodyne PUC VLP-16; (**F**) YellowScan Mapper II; (**G**) YellowScan Surveyor.

Table 7. Main parameters of some lidar sensors designed for UAS.

Manufacturer and Model	Range [m]	Weight [g]	Field of View [°]	Laser Class	Accuracy [mm]
Riegl VUX-1UAV	3–350	3500	330	1	10
Riegl VUX-240	5–1400	3800	±37.5	3R	20
Routescene UAV LidarPod	0–100	1300	(H)41, (V)360	1	(XY) 15 * (Z) 8 *
Velodyne HDL-32E	80–100	1300	(H)360, (V)+10 to −30	1	20
Velodyne PUC VLP-16	0–100	830	(H)360, (V)±15	1	30
YellowScan Mapper II	10–75	2100	100	1	(XY) 150 (Z) 50
YellowScan Surveyor	10–60	1600	360	1	50

(H) Horizontal, (V) Vertical, * *with RTK*.

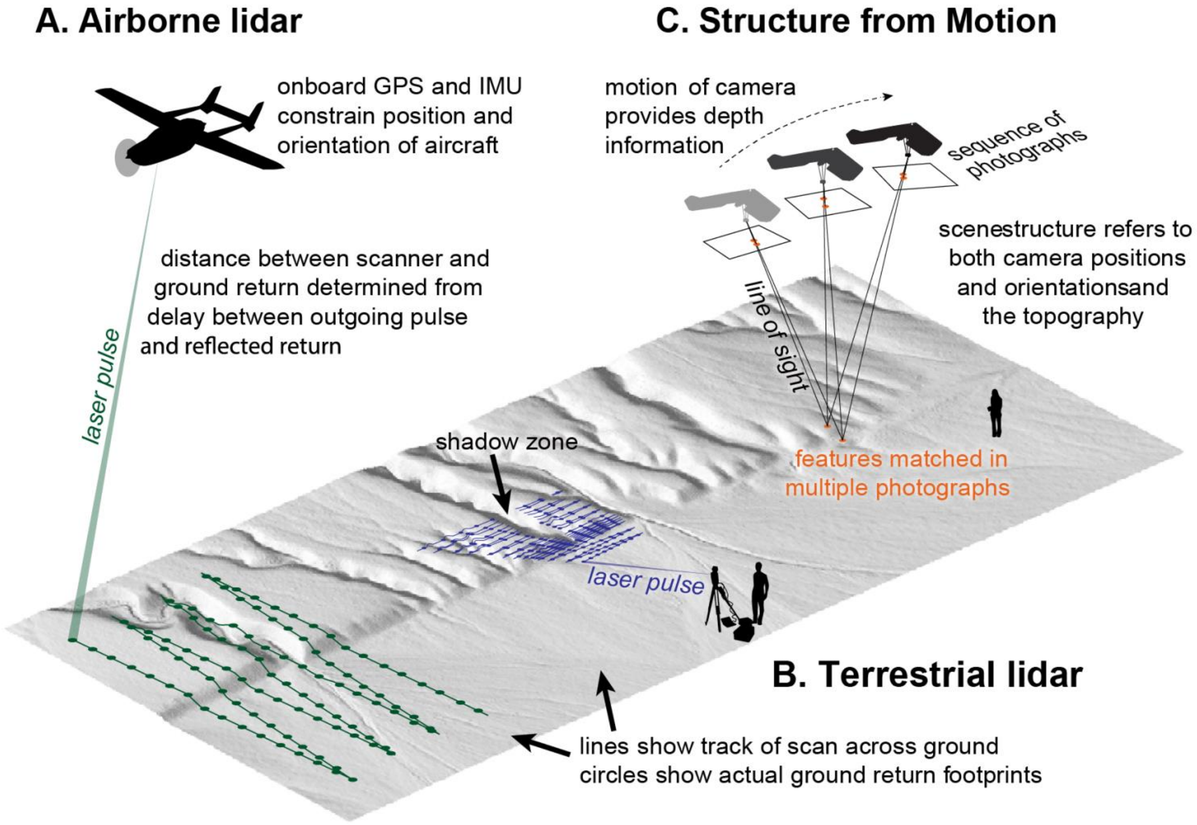

Figure 14. A schematic illustration of three methods of producing high-resolution digital topography: **A**. Airborne lidar (light detection and ranging), **B**. Terrestrial lidar, **C**. UAS-based structure from Motion (GPS—global positioning system; IMU—inertial measurement unit), modified from Johnson et al. [72].

Justyna Jeziorska, UAS for Wetland Mapping and Hydrological Modeling, Remote Sensing, 11, 2019, doi:10.3390/rs11171997

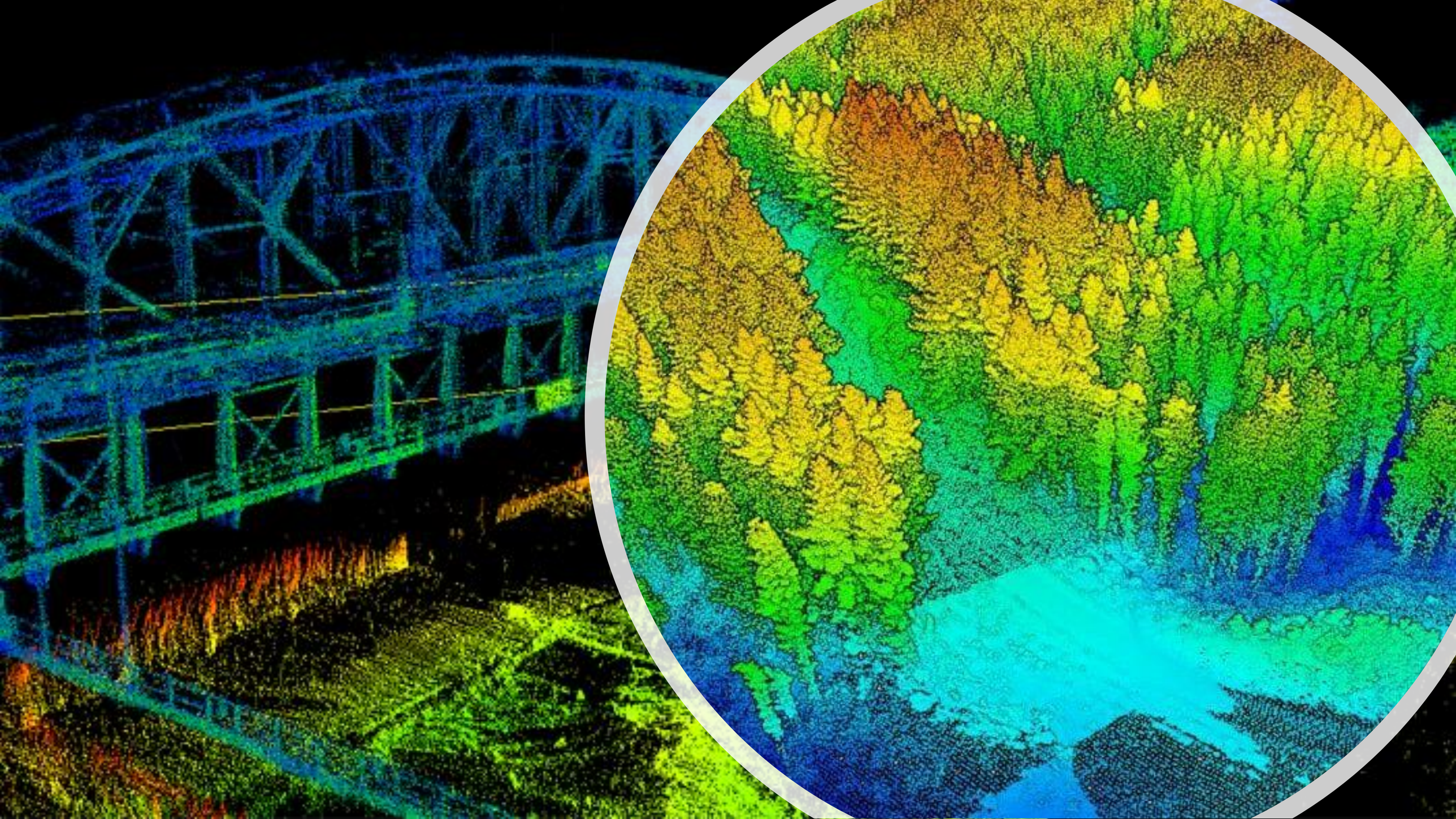

Video “Google Earth’s incredible 3D imagery, explained”

Credits to Nat and Friends YouTube channel

unite! University Network for Innovation, Technology and Engineering

U LISBOA | UNIVERSIDADE DE LISBOA

Co-funded by the Erasmus+ Programme of the European Union


Ulisses
UNITE!
University Network for Innovation, Technology and Engineering
U LISBOA
UNIVERSIDADE DE LISBOA